The phosphatase Glc7 controls eisosomal response to starvation via posttranslational modification of Pil1

Katherine M. Paine[1], Gareth J. O. Evans[1], Kamilla M. E. Laidlaw[1] and Chris MacDonald[1][2]

¹ *York Biomedical Research Institute and Department of Biology, University of York, York, UK*
² *Correspondence: Email: chris.macdonald@york.ac.uk   Tel: +44 (0) 1904 328 609*

ABSTRACT

The yeast plasma membrane (PM) is organised into specific subdomains that can regulate the activity of surface membrane proteins localised within them. Nutrient transporters actively uptake substrates in particular regions of the PM where they are also susceptible to the endocytic machinery for substrate induced degradation. However, transporters also diffuse into distinct subdomains termed eisosomes, where they are inactive for substrate uptake and are protected from endocytosis. Although most nutrient transporter populations are sorted to the vacuole for degradation during glucose starvation, a small pool are retained in eisosomes. Sequestering this small pool of transporters during nutrient stress is essential for efficient recovery from starvation following a return to replete conditions. However, the mechanisms controlling this process at a biochemical level are poorly defined. We find the core eisosome subunit Pil1, a Bin, Amphiphysin and Rvs. (BAR) domain protein involved in membrane dynamics required for eisosome biogenesis, is primarily phosphorylated by Pkh2 but that Pil1 dephosphorylation occurs during acute glucose starvation. We screened for enzyme localisation and activity to implicate the essential phosphatase Glc7 as the primary enzyme responsible for Pil1 dephosphorylation. Manipulation of *GLC7* expression correlates with Pil1 hypo/hyper phosphorylation. Furthermore, *glc7* mutants and Pil1-phosphomutants are defective in recovering from glucose starvation. We propose precise posttranslational control of Pil1 modulates nutrient transporter retention within eisosomes depending on cellular nutritional status, to maximise recovery from starvation.

INTRODUCTION

The plasma membrane (PM) of eukaryotic cells is organised into distinct domains of specific lipids and proteins (Kraft, 2013). In the budding yeast *Saccharomyces cerevisiae*, microdomains of the PM have been characterised by fluorescence microscopy and shown to house distinct protein populations (Léon and Teis, 2018). Original localisation studies distinguished between the hexose transporter Hxt1, that is uniformly dispersed across the surface and other proteins that were found in discrete, non-overlapping regions (Malínská et al., 2003). The type 2-type H⁺-ATPase Pma1 is distinct from punctate subdomains marked by the amino acid transporters Can1 and Fur4 (Grossmann et al., 2007; Malinska et al., 2004). The subdomains containing these nutrient transporters are also termed eisosomes (Walther et al., 2006). Since then, many distinct regions and spatiotemporal patterns have been observed for different proteins localised to the yeast PM (Berchtold and Walther, 2009; Grossmann et al., 2007; Heinisch et al., 2010; Murley et al., 2017; Spira et al., 2012). The punctate eisosome regions with concentrated Can1 signal were originally estimated to be membrane furrows approximately 300nm long and enriched in sterols and sphingolipids (Grossmann et al., 2007; Malínská et al., 2003; StráDalová et al., 2009). Eisosomes are formed *de novo* randomly across the PM, where they are immobilised (Moreira et al., 2009). Beyond the original proteins localised to eisosomes, many additional factors have been identified, such as core structural proteins, post-translational modifiers, tetraspan membrane proteins and uncharacterised proteins (Foderaro et al., 2017). Eisosomes have been identified in other fungal species, such as *Aspergillus nidulans* and *Ashbya gossypii* (Seger et al., 2011; Vangelatos et al., 2010), as well as various species of lichens and algae (Lee et al., 2015).

Eisosome structure and function is known to be regulated by some of these factors. Examples include the Bin, Amphiphysin and Rvs (BAR) domain proteins Pil1 and Lsp1 required for eisosome biogenesis, which are involved in binding to the PM and organising lipids during the sculpting of eisosomes (Moreira et al., 2009; Walther et al., 2006; Zhao et al., 2013; Ziółkowska et al., 2011). The eisosomal kinases Pkh1 and Pkh2 function by phosphorylating both Pil1 and Lsp1, which is required for eisosome assembly (Luo et al., 2008; Walther et al., 2007). A screen for PI(4,5)P₂ regulators revealed eisosome factors Slm1 and Slm2 also bind lipids, which are required for proper eisosomal organisation and integrate with TORC2 signalling and lipid synthesis (Audhya et al., 2004; Berchtold et al., 2012; Kamble et al., 2011; Riggi et al., 2018). Other examples of proteins required for proper eisosome assembly include Nce102, a sphingolipid sensor (Fröhlich et al., 2009; Vaskovicova et al.,

2020; Zahumenský et al., 2022), and Seg1, a stability factor that operates upstream of Pil1 (Moreira et al., 2012; Seger et al., 2011).

Many nutrient transporters diffuse in and out of eisosomes (Babst, 2019; Grossmann et al., 2008). Yeast cells uptake nutrients from their external environment through specific transporters that localise to the PM (Jack et al., 2000). Regulation of these transporters at the PM allows for nutrient acquisition to be tightly controlled in response to cellular requirements. When nutrient transporters are in eisosomes they are protected from endocytosis (Grossmann et al., 2008) and nutrient uptake activity is inhibited. For uptake of arginine, the Can1 transporter undergoes a conformational shift and moves from eisosomes to distinct regions of the PM, where it can subsequently be endocytosed (Gournas et al., 2018). A similar PM relocation mechanism is observed for the Mup1 transporter in response to methionine addition (Busto et al., 2018; Moharir et al., 2018).

Active transporters localised to the PM, like Fur4, Can1 and Mup1, undergo conformational changes in response to nutrients and are more efficiently serviced by the endocytic machinery (Gournas et al., 2017; Guiney et al., 2016; Keener and Babst, 2013). Nutrient transporter ubiquitination is the signal for trafficking through the multivesicular body pathway, where ubiquitinated proteins are recognised and packaged into intralumenal vesicles of the MVB by the endosomal sorting complex required for transport (ESCRT) apparatus (Migliano et al., 2022). Upon MVB-vacuole fusion, intraluminal vesicles containing surface proteins are deposited in the degradative environment of the vacuolar lumen. These feedback mechanisms allow degradation to avoid excessive nutrient uptake, which can be detrimental (Kaur and Bachhawat, 2007; Séron et al., 1999; Watanabe et al., 2014). This pathway is coordinated in response to nutritional cues, for example in response to nitrogen starvation, surface proteins are degraded more readily by the elevation in vacuolar sorting triggered via Rsp5 and its adaptors (MacGurn et al., 2011; Müller et al., 2015). Rsp5 mediated degradation is also upregulated in response to growth past log-phase when niacin becomes limited (MacDonald et al., 2015). Surface proteins are also degraded faster and recycled less efficiently in response to leucine starvation (Jones et al., 2012; MacDonald and Piper, 2017). A similar dual control of trafficking pathways in response to glucose starvation, which triggers surface protein degradation (Lang et al., 2014), occurs through an increase in AP180 mediated endocytosis and a decrease in Gpa1-PI3-kinase mediated recycling (Laidlaw et al., 2021; Laidlaw et al., 2022).

Some of these stress condition experiments have shown that the entire nutrient transporter population is not degraded, with at least some of the cellular pool being sequestrated in eisosomes. This has only been shown for nutrient transporters, suggesting other cargoes are degraded in response to starvation but specifically retaining a reserve pool of nutrient transporters allows efficient recovery from starvation. Unlike the response to substrate, where transporters like Can1, Fur4 and Mup1 move from eisosomes and undergo endocytosis, starvation conditions like poor nitrogen source or growth to stationary phase results in increased transporter concentration in eisosomes (Gournas et al., 2018; Moharir et al., 2018). Stress conditions trigger restructuring of eisosomes, with changes in PM tension and deepening of these structures, to better retain this reserve pool of nutrient transporters (Appadurai et al., 2020; Moharir et al., 2018; Riggi et al., 2018). Our single molecule work has shown that biophysical changes in Pil1 are observed at this time, including an increase in molecular stoichiometry and diffusion coefficients (Laidlaw et al., 2021), which might contribute to such structural alterations during stress. Furthermore, there is a physiological benefit to harbouring these nutrient transporters in eisosomes: to allow efficient recovery following a return to replete conditions. For example, the uracil transporter Fur4 that is required at the surface for efficient growth in limited uracil conditions contributes to efficient recovery following glucose starvation, in a uracil-dependent manner (Laidlaw et al., 2021; Paine et al., 2021).

The retention of nutrient transporters in response to stress is not well understood at a mechanistic level. As mentioned, phosphorylation of the core factor Pil1 by Pkh-kinases is required for eisosome biogenesis (Karotki et al., 2011; Luo et al., 2008; Walther et al., 2007). We show Pkh2 is the main kinase that regulates Pil1 phosphorylation but also that Pil1 is dephosphorylated in response to the glucose starvation conditions that trigger transporter retention. We identify Glc7 as a critical enzyme that regulates Pil1 dephosphorylation and show Glc7 activity is required for efficient recovery from starvation. Furthermore, phosphoablative and phosphomimetic Pil1 mutants are both defective in starvation recovery. We propose that the alteration of Pil1 phosphorylation modulates lipid binding to alter eisosomes, not only during biogenesis but in response to changes in nutritional conditions, allowing better retention of nutrient transporters.

RESULTS

Pkh2 is the predominant kinase that phosphorylates Pil1

It has been previously shown that Pil1 phosphorylation is ablated in a double *pkh1^ts pkh2Δ* mutant (Walther et al., 2007). To determine the contribution of Pkh1 and Pkh2 to Pil1 phosphorylation, we assessed individual deletion mutants. As Pkh3 was identified as a multicopy suppressor *pkh ^tspkh2* mutants (Inagaki et al., 1999) but has not been tested for a role in Pil1 phosphorylation, we included *pkh3Δ* mutants in this analysis. Pil1 phosphorylation status affects its migration during electrophoresis and can be visualised by immunoblot (Walther et al., 2007). Pil1 phosphorylation was assessed in all three *pkh* mutants to reveal *pkh2Δ* mutants were most defective in Pil1 phosphorylation and that *pkh1Δ* and *pkh2Δ* mutants have a small but significant defect (**Figure 1A**). We next performed localisation studies for these kinases. Although previous studies have demonstrated that over-expression of Pkh1/2 with the galactose inducible promoter *GAL1* is required for sufficient levels to localise these proteins (Roelants et al., 2002; Walther et al., 2007), we avoided this glucose-repression strategy, due to its effect on eisosome biology (Laidlaw et al., 2021). GFP-tagged kinases were instead over-expressed from the constitutive *NOP1* promoter (Weill et al., 2018) in cells co-expressing the eisosomal marker Nce102 tagged with mCherry. Only GFP-Pkh2 predominantly colocalised with Nce102-mCherry (**Figure 1B**). This small apparent contribution of Pkh1 and Pkh3 to Pil1 phosphorylation observed by immunoblot might be explained by the fact that although most cells do not localise Pkh1/3 to eisosomes, a small number of cells do (**Supplemental Figure S1A - S1B**). In further support of Pkh2 being a regulator of Pil1 phosphorylation, overexpressing Pkh2 in wild-type cells leads to a significant increase in Pil1 phosphorylation and Pkh2 plasmid expression in *pkh2Δ* cells increases Pil1 phosphorylation (**Figure 1C**). These data demonstrate that Pkh2 is the primary Pkh-family member responsible for Pil1 phosphorylation, but that Pkh1 and Pkh3 also exhibit subsidiary regulatory roles for Pil1.

Phosphorylated peptides of Pil1 have previously been identified by mass spectrometry (Albuquerque et al., 2008; Luo et al., 2008; Swaney et al., 2013; Walther et al., 2007), suggesting multiple levels of potential phosphorylation. This is also implied by the various species observed by immunoblot using an inverted step-gradient electrophoresis strategy (Laidlaw et al., 2021). Experimental work has determined several key phosphosites (Luo et al., 2008; Walther et al., 2007), which map to distinct regions of the Pil1 structure (**Figure 2A**). To ascertain if any additional kinases beyond the Pkh-family were responsible for Pil1 phosphorylation, NetPhorest analysis (Horn et al., 2014) was used to predict potential kinases for known Pil1 phosphosites (**Figure 2B**). Mutants of any high scoring kinases were tested for a role in phosphorylating Pil1 by immunoblot (**Supplemental Figure S2**). Only eight mutants showed any indication of a potential role, which was followed up quantitatively. This revealed *hog1Δ* cells lacking the yeast homologue of the mammalian MAPK p38, Hog1 (Han et al., 1994), had reduced levels of Pil1 phosphorylation. Also, depletion mutants with reduced levels of the Hippo-like kinase Cdc15 (Rock et al., 2013; Steensma et al., 1987), by virtue of a DAmP cassette (Breslow et al., 2008), showed higher levels of Pil1 phosphorylation (**Figure 2C**). This additional analysis again supports the notion that Pkh2 is the primary enzyme responsible for Pil1 phosphorylation, but that phosphorylation via other kinases may also have an impact, potentially through indirect mechanisms such as transcriptional or stress-induced control.

Pil1 is dephopshorylated in response to glucose starvation

In response to acute glucose starvation, nutrient transporters localise to eisosomes (Laidlaw et al., 2021) and are hypothesised to relocate to PM regions for nutrient uptake upon return to replete conditions (**Figure 3A**). For glucose starvation, media lacking glucose but containing the trisaccharide raffinose, which cannot be quickly metabolised (de la Fuente and Sols, 1962), is used. Upon raffinose exchange, nutrient transporters such as Mup1 concentrate to eisosomes within 10 minutes (**Figure 3B**). During the initial period of glucose starvation when nutrient transporters accumulate in eisosomes, we observe rapid Pil1 dephosphorylation (**Figure 3C**). We also observe significant glucose induced dephosphorylation in *pkh1Δ*, again suggesting it is not a key regulator of Pil1 phosphorylation (**Supplemental Figure S3**).

We hypothesise that Pil1 dephosphorylation in response to glucose starvation plays a role in the ability of eisosomes to sequester nutrient transporters in response to glucose starvation. In *Saccharomyces cerevisiae* 43 phosphatases have been identified (Offley and Schmidt, 2019), of which 39 are non-essential and 4 are essential. To identify the phosphatase(s) responsible for Pil1 dephosphorylation, we screened mutants of all phosphatase enzymes for their activity in glucose and raffinose conditions (**Figure 4A**). Pil1 phosphorylation status was assessed in null mutants (Δ) lacking non-essential phosphatases or with reduced expression of essential phosphatases, by virtue of a DaMP cassette (Breslow et al., 2008). Mutants were scored based on defects in Pil1 dephosphorylation (**Figure 4B**). This screen revealed 7 top scoring phosphatase mutants selected for further quantitative analysis (**Figure 5A - 5B**). Next, we assessed the localisation of GFP tagged phosphatases at mid-log phase and stationary phase (**Figure 5C, Supplemental Figure S4**). We included stationary phase as a nutritional stress associated with eisosome transporter retention (Gournas et al., 2018).

This confirmed a range of localisations, many to the nucleus and cytoplasm but also Ppn2 at the vacuole and Ptc5 at the mitochondria (Breker et al., 2013). Interestingly, we also observed several GFP tagged phosphatases that had changes in localisation following growth to stationary phase, including Sdp1, Ptc5, and Nem1. Although GFP-Msg5 and GFP-Siw14 fusions localised to the periphery upon growth to stationary phase, deletion of these mutants had no impact on Pil1 phosphorylation, so we assume this peripheral localisation is not related to eisosome regulation. However, GFP-Glc7 showed significant peripheral punctate localisation in both growth conditions, in addition to localisation to the mid-body, the cytoplasm and the nucleus (Bloecher and Tatchell, 2000; Breker et al., 2013). The only phosphatase that showed significant localisation to the cell periphery and that exhibited defects in phosphorylation upon mutation, was Glc7.

Glc7 functions in regulation of Pil1

Glc7 is an essential phosphatase (Clotet et al., 1991; Feng et al., 1991) that has been previously show to function in glucose related pathways, where it acts with its regulatory subunit Reg1 (Tu and Carlson, 1995) and bud neck formation (Larson et al., 2008), amongst other roles in the cell. We confirmed that $glc7^{DAmP}$ results in reduced dephosphorylation of Pil1 in both glucose replete and glucose starvation conditions (**Figure 6A**). Intriguingly, these effects are independent of Reg1, as $reg1\Delta$ cells exhibit slightly increased levels of Pil1 dephosphorylation (**Figure 6B - 6C**). As a complementary approach to test the role of Glc7 in Pil1 phosphorylation we altered *GLC7* expression levels using a YETI (Yeast Estradiol with Titratable Induction) strain (Arita et al., 2021) which allows modulation using ß-estradiol concentrations (**Figure 6D**). We reveal *GLC7* expression correlates with Pil1 phosphorylation, with 100 mM ß-estradiol induced over-expression of *GLC7* reducing Pil1 phosphorylation and removing ß-estradiol entirely increasing phosphorylated species (**Figure 6E - 6F**). This analysis demonstrates the YETI system in media lacking ß-estradiol for 6-hours has a more pronounced decrease in *GLC7* expression than $glc7^{DAmP}$. Collectively, this suggests the role of Glc7 in Pil1 phosphorylation might be direct, so we sought to test if Glc7 colocalises to eisosomes marked with Nce102-mCherry. However, neither steady state or time lapse imaging in glucose and raffinose media revealed large amounts of Glc7 localisation to eisosomes, but there were often small regions of colocalisation in a restricted number of eisosomes (**Figure 6G - 6H**).

Phosphorylation of Pil1 is important for recovery after glucose starvation

Having implicated Glc7 in Pil1 dephosphorylation that occurs during glucose starvation, we next wanted to test if this regulation controls Pil1 function in starvation recovery. Previous studies have assessed the phosphorylation profile of various Pil1 mutants with mutation of 8 verified phosphosites (Luo et al., 2008; Walther et al., 2007). We generated phosphoablative (changed to alanine, 8A) and phosphomimetic (changed to aspartate, 8D) versions of Pil1 at these phosphosites (**Figure 7A**). Western blotting confirmed that the 8A and 8D mutations resulted in Pil1 migrating not as a doublet, but as a single band, with faster migration of the phosphoablative Pil1-8A-mGFP and slower migration of the phosphomimetic Pil1-8D-mGFP fusion (**Figure 7B**). Fluorescence microscopy of GFP tagged Pil1 versions showed both 8A and 8D expressing strains exhibited an altered localisation phenotype compared to wild-type cells (**Figure 7C**), as previously documented for phosphomutants of Pil1. This confirms what was previously shown for phosphomimetic and ablative mutants (Luo et al., 2008; Walther et al., 2007). We quantified these differences (**Supplemental Figure S5**) revealing both mutants have fewer eisosomes per cell compared to wild type (**Figure 7D**). Furthermore, both ablative and mimetic mutants exhibit more cytoplasmic signal (**Figure 7E**). This analysis showed a more pronounced defect in eisosome number and levels for Pil1-8D-mGFP than Pil1-8A-mGFP.

To test if Pil1 phosphomutants were functional in starvation recovery, we used an assay that tracks recovery growth following 2 hours glucose starvation (Laidlaw et al., 2021). This assay cultures cells in minimal media, which shows no growth differences between wild-type and phosphomutants of Pil1 (**Figure 7F**). We do note that in rich YPD media, the Pil1-8A and Pil1-8D mutants have defects in growth at early time points, potentially explained by a connection between nutritional status and Pil1 phosphorylation. However, unlike comparable growth under non-stress conditions, we find that both Pil1-8A and Pil1-8D mutations are defective in recovery growth (**Figure 7G - 7H**). This suggests phosphoregulation of Pil1 is required to modify eisosomes that sequester nutrient transporters during nutritional challenges.

Pil1 mutants that cannot modulate phosphorylation status are impaired in their ability to recover from starvation, and Pkh2 and Glc7 are required for these post translational modifications. Therefore, our model would predict that these enzymes are also required to efficiently sequester nutrient transporters in eisosomes, and for full recovery following starvation. We have previously shown that $pkh2\Delta$ mutants have reduced retention of nutrient transporters and an attenuated recovery following glucose starvation (Laidlaw et al., 2021). Similarly, $glc7^{DAmP}$ cells with reduced levels of *GLC7* have reduced eisosomal localisation of the methionine permease Mup1 tagged with GFP, in both glucose replete conditions and following a brief incubation with raffinose (**Figure 8A**). Growth assays on both rich and minimal media show that $glc7^{DAmP}$ cell growth is comparable to wild-type

cells that are not exposed to starvation conditions (**Figure 8B**). However, recovery growth of $glc7^{DAmP}$ mutants following 2 hours of glucose starvation is significantly hampered (**Figure 8C and D**).

DISCUSSION

The organisation of the yeast PM is very complex with a multitude of possible surface localisation patterns known for both integral membrane proteins and surface associated factors (Spira et al., 2012). Since the discovery of the eisosome subdomain, progress has been made in understanding the formation and biological function of these structures, particularly in response to cellular stress (Babst, 2019; Moseley, 2018). The discovery that Pil1 and Lsp1, and their phosphorylation by the Pkh-family kinases, are required for proper eisosome biogenesis (Walther et al., 2007; Walther et al., 2006) suggests post-translational modification of core components could regulate the eisosome environment. Pkh1 and Pkh2 were originally identified as homologues of human and *Drosophila* 3-phosphoinositide-dependent protein kinase-1 (PDK1) that are essential for viability (Casamayor et al., 1999). As this work showed the double *pkh1Δ pkh2Δ* yeast mutant was inviable, a double mutant with a temperature sensitive allele of *PKH1* (D398G) and deletion of *PKH2,* termed *pkh1^{ts} pkh2Δ*, was used to study kinase signalling pathways (Inagaki et al., 1999). This double *pkh1^{ts} pkh2Δ* mutant also revealed an early association of Pkh-kinases with endocytosis, with this strain impaired for internalization from the PM (Friant et al., 2001). Due to the shared essential function of Pkh1 and Pkh2, the double mutant was the most logical strain to test effects on biogenesis of eisosomes upon their discovery (Walther et al., 2007; Walther et al., 2006). However, we find Pkh2 is predominantly responsible for phosphorylating Pil1 with only minor roles for Pkh1 or indeed the related kinase Pkh3 (**Figure 1A**). We also did not observe substantial amounts of Pkh1 or Pkh3 at eisosomes. One key difference to our work and previous localisation of Pkh1 to eisosomes (Walther et al., 2007) is that we did not use the *GAL1* promoter for over-expression, so it may be that the glucose starvation stress of galactose induction media alters Pkh1 localisation or the eisosome environment. Further exploring other potential kinase and phosphosites did suggest the Hog1 and Cdc15 kinases might also exhibit small roles regulating Pil1, but these effects were also relatively modest compared with Pkh2 (**Figure 2**). Of note, the phosphoshift seen for Pil1 is mainly caused by phosphorylation at S273 (Walther et al., 2007), as the focus of this work was not kinase regulation future work using alternative approaches may better clarify the role of alternative kinases in Pil1 regulation.

The finding that extracellular stress results in the accumulation of nutrient transporters in eisosome compartments, which deepen to facilitate this process, suggests a key role of eisosomes is related to nutritional uptake following stress (Appadurai et al., 2020; Gournas et al., 2018). We have previously shown the specific stress of acute glucose starvation (0-2 hours) results in concentration of the nutrient transporter Mup1 to eisosomes. As eisosomal mutants fail to properly retain nutrient transporters and fail to recover efficiently from starvation (Laidlaw et al., 2021), we propose acute glucose starvation modulates eisosomes to better harbour transporters for recovery. We find the core eisosomal Pil1 is rapidly dephosphorylated during the same acute glucose starvation period (**Figure 3**). This led to the model that the phosphorylation status of Pil1 is important for reorganisation of existing eisosomes during cargo retention, in addition to its established role in eisosome biogenesis. These functions could be one and the same at the molecular level, with changes in phosphorylation and charge of Pil1 having the potential to affect its lipid binding/sculping capacity. As membrane bending effects of other BAR domain proteins are known to be affected by disordered regions (Busch et al., 2015; Zeno et al., 2018), it is conceivable that phosphorylation can alter the biophysical properties of eisosomes.

To identify possible regulators of Pil1 dephosphorylation that might regulate eisosomes during stress, we systematically screened mutants of all encoded yeast phosphatases, in both glucose replete and starved conditions. This effort implicated a role for Glc7, an essential Type 1 Serine/Threonine protein phosphatase (Cannon et al., 1994; Peng et al., 1990). We confirmed Glc7 regulates Pil1 by decreasing Glc7 levels using a Decreased Abundance by mRNA Perturbation (DAmP) method (Breslow et al., 2008) and a Yeast Estradiol with Titratable Induction (YETI) strategy (Arita et al., 2021), both of which showed elevated levels of Pil1 phosphorylation (**Figure 6**). This latter approach also allowed over-expression of *GLC7*, which resulted in further Pil1 dephosphorylation. Although Glc7 was the only phosphatase to regulate Pil1 phosphorylation in addition to localising to the cell periphery (**Figure 5**), we only observed small levels of colocalisation of Glc7 with Pil1. Glc7 has several roles in the cell including, growth, mitosis, transcription, stabilisation of emerging buds, glycogen metabolism and ion homeostasis (Feng et al., 1991; Hisamoto et al., 1995; Kozubowski et al., 2003; Peggie et al., 2002; Sanz et al., 2004; Williams-Hart et al., 2002), which we corroborate with expected localisations at the bud-neck, nucleus and cytoplasm. It may be that at steady state very little Glc7 is required for eisosome maintenance, and this may be achieved via a transient interaction, either direct or indirect via accessory proteins.

Glc7 having a role in eisosomal modulation during glucose starvation is conceptually consistent with many studies demonstrating that Glc7 integrates with transcriptional repression in response to glucose availability, via Snf1 and downstream factors (Sanz et al., 2000; Tu and Carlson, 1994). However, as the

changes we observe in both Pil1 dephosphorylation and transporter retention are very rapid, we assume these effects are not mediated at the transcriptional level. In further support of this idea, the regulatory subunit Reg1, which is required for many transcriptional related Glc7-activities (Alms et al., 1999; Cui et al., 2004; Dombek et al., 1999), showed no increase in phosphorylated Pil1 species upon its deletion (**Figure 6B - 6C**). We did note a small but significant decrease in Pil1 phosphorylation in *reg1*Δ mutants, which could be explained by Glc7 being liberated from Reg1-mediated commitments, and more available to further dephosphorylate Pil1. Nonetheless, the fact that Glc7 is robustly associated with glucose metabolism via distinct mechanisms suggests there may be more complexity to the cellular response to carbon source availability.

The findings that *glc7* mutants are defective for transporter retention and recovery from starvation (**Figure 8**) is consistent with dephosphorylation of Pil1 during glucose starvation being the responsible biochemical driver of this response. Cells lacking the primary Pil1 kinase Pkh2 (*pkh2*Δ) are defective in recovery from glucose starvation (Laidlaw et al., 2021), as are both phosphomimetic and phosphoablative mutants of Pil1 (**Figure 7**). Collectively this implies that hyper- or hypo-phosphorylated Pil1 are not locked in a biochemical state that maximises eisosomal retention of transporters, but rather the fine-tuning of Pil1 phosphorylation is required to better harbour transporters acutely in response to nutritional stress. This mechanism could be important for understanding metabolic response of yeast to varying nutrient conditions, including pathogenic fungi (Rutherford et al., 2019). Beyond this, the role of post-translational modifications to membrane interacting proteins from other structures and compartments throughout eukaryotic cells could inform future biochemical and biophysical experimentation and understanding.

METHODS

Reagents
Supplemental Table T2 documents yeast strains used in this study.

Cell culture
Yeast cells were routinely grown in YPD (1% yeast extract, 2% peptone, 2% dextrose) or synthetic complete (SC) minimal media (2% glucose, 0.675% yeast nitrogen base without amino acids, plus appropriate amino acid dropouts for plasmid selection) (Formedium, Norfolk, UK). 2% Glucose was routinely used, where stated 4% glucose was used. Cells were subjected to glucose starvation using 2% raffinose rather than glucose as described previously (Laidlaw et al., 2021). Plasmid pCM1054 is a 2µ over-expression plasmid for Pkh2 (Jones et al., 2008) used in **Figure 1C** and plasmid pCM264 is *CEN* based pPR315 expression vector containing Mup1-GFP under control of its endogenous promoter (Stringer and Piper, 2011) used in **Figure 3B** and **Figure 8A**.

Mating of yeast strains
Haploid BY4741 mat**a** yeast strains encoding *URA3*-GFP-tagged Pkh-family kinases (Weill et al., 2018) were mated with BY4742 Matα modified at the *NCE102* locus (*nce102-mCherry-his5^{+}*) on YPD rich media overnight. Single diploid colonies were isolated on media lacking uracil and histidine and confirmed by fluorescence microscopy.

Immunoblotting
Strains were grown to mid-log phase and equivalent volumes were harvested or starved for glucose with raffinose treatment prior to harvesting. Cells were treated to 0.2 N NaOH for 5 minutes prior to resuspension in lysis buffer (8 M urea, 10% glycerol, 50 mM Tris-HCl pH 6.8, 5% SDS, 0.1 % bromophenol blue and 10% 2-mercaptoethanol). SDS-PAGE was used to resolve proteins which were then transferred to a nitrocellulose membrane using the iBlot dry transfer system (Invitrogen). Ponceau S strain was used to confirm successful transfer and equal loading. Membranes were probed with antibodies stated and visualised using enhanced chemiluminescence (ECL) Super Signal Pico Plus (Thermo) and captured using a ChemiDoc Imager (Bio-Rad).

Confocal microscopy
Yeast cells expressing fluorescently tagged proteins were grown to mid-log phase (unless stated) and then visualised in minimal media at room temperature on Zeiss laser scanning confocal instruments (Zeiss LSM880 or Zeiss 980) using a 63x/1.4 objective lens. GFP was excited using a 488nm laser and emission collected from 495 to 500 nm and mCherry was excited using the 561nm laser and emission collected from 570 – 620 nm using an Airyscan (LSM880) or Airyscan 2 (LSM980) detector. Images were captured sequentially to minimise any potential bleedthrough and processed using Zeiss Zen software standard airyscan algorithm and modified for publication using ImageJ software (NIH).

Recovery Growth Assays
Equivalent volumes of cells were harvested from mid-log cultures and washed three times with raffinose media before being resuspended in raffinose media and incubated in a shaking incubator at 30°C for 2 hours. Equivalent volumes of the raffinose starved cells were harvested and washed three times with glucose media before being resuspended in 100 µl of glucose media. This was added to 3 ml of glucose media and absorbance at OD_{600} was measured to obtain time point 0. Subsequent OD_{600} measurements were taken every hour using a plate reader (Thermo Scientific) and normalised to wild-type.

Spot Growth Assays
Equivalent volumes of cells at mid-log phase were harvested and a 10-fold serial dilution was created and spotted onto indicated plates. Plates were incubated at 30 °C and images were captured at indicated time-points using a scanner (Epson).

Bioinformatic and Statistical analyses
Prediction of kinase consensus motifs in Pil1 was undertaken by submitting the Pil1 amino acid sequence to the yeast database in Netphorest (Horn et al., 2014) and experimentally determined phosphosites (Luo et al., 2008; Walther et al., 2007) were selected for analysis. The results were filtered with a minimum phosphorylation probability score of 0.1. Unpaired Student's *t*-tests were performed using GraphPad Prism v8.3.1. to compare the statistical significance between experimental conditions, with p values in **Supplemental Table T3**. An asterisk (*) is used to denote significance.

ACKNOWLEDGMENTS

DECLARATION OF INTERESTS
The authors declare no competing interests.

REFERENCES

Albuquerque, C.P., M.B. Smolka, S.H. Payne, V. Bafna, J. Eng, and H. Zhou. 2008. A multidimensional chromatography technology for in-depth phosphoproteome analysis. *Mol Cell Proteomics*. 7:1389-1396.

Alms, G.R., P. Sanz, M. Carlson, and T.A. Haystead. 1999. Reg1p targets protein phosphatase 1 to dephosphorylate hexokinase II in Saccharomyces cerevisiae: characterizing the effects of a phosphatase subunit on the yeast proteome. *Embo j*. 18:4157-4168.

Appadurai, D., L. Gay, A. Moharir, M.J. Lang, M.C. Duncan, O. Schmidt, D. Teis, T.N. Vu, M. Silva, E.M. Jorgensen, and M. Babst. 2020. Plasma membrane tension regulates eisosome structure and function. *Mol Biol Cell*. 31:287-303.

Arita, Y., G. Kim, Z. Li, H. Friesen, G. Turco, R.Y. Wang, D. Climie, M. Usaj, M. Hotz, E.H. Stoops, A. Baryshnikova, C. Boone, D. Botstein, B.J. Andrews, and R.S. McIsaac. 2021. A genome-scale yeast library with inducible expression of individual genes. *Mol Syst Biol*. 17:e10207.

Audhya, A., R. Loewith, A.B. Parsons, L. Gao, M. Tabuchi, H. Zhou, C. Boone, M.N. Hall, and S.D. Emr. 2004. Genome-wide lethality screen identifies new PI4,5P2 effectors that regulate the actin cytoskeleton. *Embo j*. 23:3747-3757.

Babst, M. 2019. Eisosomes at the intersection of TORC1 and TORC2 regulation. *In* Traffic. Vol. 20. Blackwell Munksgaard. 543-551.

Berchtold, D., M. Piccolis, N. Chiaruttini, I. Riezman, H. Riezman, A. Roux, T.C. Walther, and R. Loewith. 2012. Plasma membrane stress induces relocalization of Slm proteins and activation of TORC2 to promote sphingolipid synthesis. *Nat Cell Biol*. 14:542-547.

Berchtold, D., and T.C. Walther. 2009. TORC2 plasma membrane localization is essential for cell viability and restricted to a distinct domain. *Molecular biology of the cell*. 20:1565-1575.

Bloecher, A., and K. Tatchell. 2000. Dynamic localization of protein phosphatase type 1 in the mitotic cell cycle of Saccharomyces cerevisiae. *J Cell Biol*. 149:125-140.

Breker, M., M. Gymrek, and M. Schuldiner. 2013. A novel single-cell screening platform reveals proteome plasticity during yeast stress responses. *J Cell Biol*. 200:839-850.

Breslow, D.K., D.M. Cameron, S.R. Collins, M. Schuldiner, J. Stewart-Ornstein, H.W. Newman, S. Braun, H.D. Madhani, N.J. Krogan, and J.S. Weissman. 2008. A comprehensive strategy enabling high-resolution functional analysis of the yeast genome. *Nature Methods*. 5:711-718.

Busch, D.J., J.R. Houser, C.C. Hayden, M.B. Sherman, E.M. Lafer, and J.C. Stachowiak. 2015. Intrinsically disordered proteins drive membrane curvature. *Nature Communications*. 6:7875.

Busto, J.V., A. Elting, D. Haase, F. Spira, J. Kuhlman, M. Schäfer-Herte, and R. Wedlich-Söldner. 2018. Lateral plasma membrane compartmentalization links protein function and turnover. *The EMBO Journal*. 37.

Cannon, J.F., J.R. Pringle, A. Fiechter, and M. Khalil. 1994. Characterization of glycogen-deficient glc mutants of Saccharomyces cerevisiae. *Genetics*. 136:485-503.

Casamayor, A., P.D. Torrance, T. Kobayashi, J. Thorner, and D.R. Alessi. 1999. Functional counterparts of mammalian protein kinases PDK1 and SGK in budding yeast. *Current Biology*. 9:186-197.

Clotet, J., F. Posas, A. Casamayor, I. Schaaff-Gerstenschläger, and J. Ariño. 1991. The gene DIS2S1 is essential in Saccharomyces cerevisiae and is involved in glycogen phosphorylase activation. *Curr Genet*. 19:339-342.

Cui, D.Y., C.R. Brown, and H.L. Chiang. 2004. The type 1 phosphatase Reg1p-Glc7p is required for the glucose-induced degradation of fructose-1,6-bisphosphatase in the vacuole. *J Biol Chem*. 279:9713-9724.

de la Fuente, G., and A. Sols. 1962. Transport of sugars in yeasts. II. Mechanisms of utilization of disaccharides and related glycosides. *Biochimica et biophysica acta*. 56:49-62.

Dombek, K.M., V. Voronkova, A. Raney, and E.T. Young. 1999. Functional analysis of the yeast Glc7-binding protein Reg1 identifies a protein phosphatase type 1-binding motif as essential for repression of ADH2 expression. *Mol Cell Biol*. 19:6029-6040.

Feng, Z.H., S.E. Wilson, Z.Y. Peng, K.K. Schlender, E.M. Reimann, and R.J. Trumbly. 1991. The yeast GLC7 gene required for glycogen accumulation encodes a type 1 protein phosphatase. *J Biol Chem*. 266:23796-23801.

Foderaro, J.E., L.M. Douglas, and J.B. Konopka. 2017. MCC/Eisosomes Regulate Cell Wall Synthesis and Stress Responses in Fungi. *J Fungi (Basel)*. 3.

Friant, S., R. Lombardi, T. Schmelzle, M.N. Hall, and H. Riezman. 2001. Sphingoid base signaling via Pkh kinases is required for endocytosis in yeast. *The EMBO journal*. 20:6783-6792.

Fröhlich, F., K. Moreira, P.S. Aguilar, N.C. Hubner, M. Mann, P. Walter, and T.C. Walther. 2009. A genome-wide screen for genes affecting eisosomes reveals Nce102 function in sphingolipid signaling. *Journal of Cell Biology*. 185:1227-1242.

Gournas, C., S. Gkionis, M. Carquin, L. Twyffels, D. Tyteca, and B. André. 2018. Conformation-dependent partitioning of yeast nutrient transporters into starvation-protective membrane domains. *Proceedings of the National Academy of Sciences of the United States of America*. 115:E3145-E3154.

Gournas, C., E. Saliba, E.-M. Krammer, C. Barthelemy, M. Prévost, and B. André. 2017. Transition of yeast Can1 transporter to the inward-facing state unveils an α-arrestin target sequence promoting its ubiquitylation and endocytosis. *Molecular Biology of the Cell*. 28:2819-2832.

Grossmann, G., J. Malinsky, W. Stahlschmidt, M. Loibl, I. Weig-Meckl, W.B. Frommer, M. Opekarová, and W. Tanner. 2008. Plasma membrane microdomains regulate turnover of transport proteins in yeast. *Journal of Cell Biology*. 183:1075-1088.

Grossmann, G., M. Opekarová, J. Malinsky, I. Weig-Meckl, and W. Tanner. 2007. Membrane potential governs lateral segregation of plasma membrane proteins and lipids in yeast. *EMBO Journal*. 26:1-8.

Guiney, E.L., T. Klecker, and S.D. Emr. 2016. Identification of the endocytic sorting signal recognized by the Art1-Rsp5 ubiquitin ligase complex. *Mol Biol Cell*. 27:4043-4054.

Han, J., J.D. Lee, L. Bibbs, and R.J. Ulevitch. 1994. A MAP kinase targeted by endotoxin and hyperosmolarity in mammalian cells. *Science*. 265:808-811.

Heinisch, J.J., V. Dupres, S. Wilk, A. Jendretzki, and Y.F. Dufrêne. 2010. Single-molecule atomic force microscopy reveals clustering of the yeast plasma-membrane sensor Wsc1. *PLoS One*. 5:e11104.

Hisamoto, N., D.L. Frederick, K. Sugimoto, K. Tatchell, and K. Matsumoto. 1995. The EGP1 gene may be a positive regulator of protein phosphatase type 1 in the growth control of Saccharomyces cerevisiae. *Mol Cell Biol*. 15:3767-3776.

Horn, H., E.M. Schoof, J. Kim, X. Robin, M.L. Miller, F. Diella, A. Palma, G. Cesareni, L.J. Jensen, and R. Linding. 2014. KinomeXplorer: an integrated platform for kinome biology studies. *Nature Methods*. 11:603-604.

Inagaki, M., T. Schmelzle, K. Yamaguchi, K. Irie, M.N. Hall, and K. Matsumoto. 1999. PDK1 homologs activate the Pkc1-mitogen-activated protein kinase pathway in yeast. *Mol Cell Biol*. 19:8344-8352.

Jack, D.L., I.T. Paulsen, and Saier, Jr. 2000. The amino acid/polyamine/organocation (APC) superfamily of transporters specific for amino acids, polyamines and organocations. *Microbiology*. 146:1797-1814.

Jones, C.B., E.M. Ott, J.M. Keener, M. Curtiss, V. Sandrin, and M. Babst. 2012. Regulation of membrane protein degradation by starvation-response pathways. *Traffic (Copenhagen, Denmark)*. 13:468-482.

Jones, G.M., J. Stalker, S. Humphray, A. West, T. Cox, J. Rogers, I. Dunham, and G. Prelich. 2008. A systematic library for comprehensive overexpression screens in Saccharomyces cerevisiae. *Nat Methods*. 5:239-241.

Kamble, C., S. Jain, E. Murphy, and K. Kim. 2011. Requirements of Slm proteins for proper eisosome organization, endocytic trafficking and recycling in the yeast Saccharomyces cerevisiae. *J Biosci*. 36:79-96.

Karotki, L., J.T. Huiskonen, C.J. Stefan, N.E. Ziółkowska, R. Roth, M.A. Surma, N.J. Krogan, S.D. Emr, J. Heuser, K. Grünewald, and T.C. Walther. 2011. Eisosome proteins assemble into a membrane scaffold. *J Cell Biol*. 195:889-902.

Kaur, J., and A.K. Bachhawat. 2007. Yct1p, a novel, high-affinity, cysteine-specific transporter from the yeast Saccharomyces cerevisiae. *Genetics*. 176:877-890.

Keener, J.M., and M. Babst. 2013. Quality Control and Substrate-Dependent Downregulation of the Nutrient Transporter Fur4. *Traffic*. 14:412-427.

Kozubowski, L., H. Panek, A. Rosenthal, A. Bloecher, D.J. DeMarini, and K. Tatchell. 2003. A Bni4-Glc7 phosphatase complex that recruits chitin synthase to the site of bud emergence. *Mol Biol Cell*. 14:26-39.

Kraft, M.L. 2013. Plasma membrane organization and function: moving past lipid rafts. *Mol Biol Cell*. 24:2765-2768.

Laidlaw, K.M.E., D.D. Bisinski, S. Shashkova, K.M. Paine, M.A. Veillon, M.C. Leake, and C. MacDonald. 2021. A glucose-starvation response governs endocytic trafficking and eisosomal retention of surface cargoes in budding yeast. *Journal of Cell Science*. 134:jcs.257733-jcs.257733.

Laidlaw, K.M.E., K.M. Paine, D.D. Bisinski, G. Calder, K. Hogg, S. Ahmed, S. James, P.J. O'Toole, and C. MacDonald. 2022. Endosomal cargo recycling mediated by Gpa1 and phosphatidylinositol 3-kinase is inhibited by glucose starvation. *Molecular biology of the cell*. 33.

Lang, M.J., J.Y. Martinez-Marquez, D.C. Prosser, L.R. Ganser, D. Buelto, B. Wendland, and M.C. Duncan. 2014. Glucose starvation inhibits autophagy via vacuolar hydrolysis and induces plasma membrane internalization by down-regulating recycling. *Journal of Biological Chemistry*. 289:16736-16747.

Larson, J.R., J.P. Bharucha, S. Ceaser, J. Salamon, C.J. Richardson, S.M. Rivera, and K. Tatchell. 2008. Protein phosphatase type 1 directs chitin synthesis at the bud neck in Saccharomyces cerevisiae. *Mol Biol Cell*. 19:3040-3051.

Lee, J.H., J.E. Heuser, R. Roth, and U. Goodenough. 2015. Eisosome ultrastructure and evolution in fungi, microalgae, and lichens. *Eukaryotic Cell*. 14:1017-1042.

Léon, S., and D. Teis. 2018. Functional patchworking at the plasma membrane. *Embo j*. 37.

Luo, G., A. Gruhler, Y. Liu, O.N. Jensen, and R.C. Dickson. 2008. The sphingolipid long-chain base-Pkh1/2-Ypk1/2 signaling pathway regulates eisosome assembly and turnover. *Journal of Biological Chemistry*. 283:10433-10444.

MacDonald, C., J.A. Payne, M. Aboian, W. Smith, D.J. Katzmann, and R.C. Piper. 2015. A Family of Tetraspans Organizes Cargo for Sorting into Multivesicular Bodies. *Developmental Cell*. 33:328-342.

MacDonald, C., and R.C. Piper. 2017. Genetic dissection of early endosomal recycling highlights a TORC1-independent role for Rag GTPases. *Journal of Cell Biology*. 216:3275-3290.

MacGurn, J.A., P.C. Hsu, M.B. Smolka, and S.D. Emr. 2011. TORC1 regulates endocytosis via Npr1-mediated phosphoinhibition of a ubiquitin ligase adaptor. *Cell*. 147:1104-1117.

Malinska, K., J. Malinsky, M. Opekarova, and W. Tanner. 2004. Distribution of Can1p into stable domains reflects lateral protein segregation within the plasma membrane of living S. cerevisiae cells. *Journal of Cell Science*. 117:6031-6041.

Malínská, K., J. Malínský, M. Opekarová, and W. Tanner. 2003. Visualization of Protein Compartmentation within the Plasma Membrane of Living Yeast Cells. *Molecular Biology of the Cell*. 14:4427-4436.

Migliano, S.M., E.M. Wenzel, and H. Stenmark. 2022. Biophysical and molecular mechanisms of ESCRT functions, and their implications for disease. *Current Opinion in Cell Biology*. 75:102062.

Moharir, A., L. Gay, D. Appadurai, J. Keener, and M. Babst. 2018. Eisosomes are metabolically regulated storage compartments for APC-type nutrient transporters. *Molecular Biology of the Cell*. 29:2113-2127.

Moreira, K.E., S. Schuck, B. Schrul, F. Fröhlich, J.B. Moseley, T.C. Walther, and P. Walter. 2012. Seg1 controls eisosome assembly and shape. *J Cell Biol*. 198:405-420.

Moreira, K.E., T.C. Walther, P.S. Aguilar, and P. Walter. 2009. Pil1 Controls Eisosome Biogenesis. *Molecular Biology of the Cell*. 20:809-818.

Moseley, J.B. 2018. Eisosomes. *Curr Biol*. 28:R376-r378.

Müller, M., O. Schmidt, M. Angelova, K. Faserl, S. Weys, L. Kremser, T. Pfaffenwimmer, T. Dalik, C. Kraft, Z. Trajanoski, H. Lindner, and D. Teis. 2015. The coordinated action of the MVB pathway and autophagy ensures cell survival during starvation. *eLife*. 4:e07736.

Murley, A., J. Yamada, B.J. Niles, A. Toulmay, W.A. Prinz, T. Powers, and J. Nunnari. 2017. Sterol transporters at membrane contact sites regulate TORC1 and TORC2 signaling. *J Cell Biol*. 216:2679-2689.

Offley, S.R., and M.C. Schmidt. 2019. Protein phosphatases of Saccharomyces cerevisiae. *Curr Genet*. 65:41-55.

Paine, K.M., G.B. Ecclestone, and C. Macdonald. 2021. Fur4 mediated uracil-scavenging to screen for surface protein regulators. *bioRxiv*:2021.2005.2027.445995-442021.445905.445927.445995.

Peggie, M.W., S.H. MacKelvie, A. Bloecher, E.V. Knatko, K. Tatchell, and M.J. Stark. 2002. Essential functions of Sds22p in chromosome stability and nuclear localization of PP1. *J Cell Sci*. 115:195-206.

Peng, Z.Y., R.J. Trumbly, and E.M. Reimann. 1990. Purification and characterization of glycogen synthase from a glycogen-deficient strain of Saccharomyces cerevisiae. *J Biol Chem*. 265:13871-13877.

Riggi, M., K. Niewola-Staszkowska, N. Chiaruttini, A. Colom, B. Kusmider, V. Mercier, S. Soleimanpour, M. Stahl, S. Matile, A. Roux, and R. Loewith. 2018. Decrease in plasma membrane tension triggers PtdIns(4,5)P(2) phase separation to inactivate TORC2. *Nat Cell Biol*. 20:1043-1051.

Rock, J.M., D. Lim, L. Stach, R.W. Ogrodowicz, J.M. Keck, M.H. Jones, C.C. Wong, J.R. Yates, 3rd, M. Winey, S.J. Smerdon, M.B. Yaffe, and A. Amon. 2013. Activation of the yeast Hippo pathway by phosphorylation-dependent assembly of signaling complexes. *Science*. 340:871-875.

Roelants, F.M., P.D. Torrance, N. Bezman, and J. Thorner. 2002. Pkh1 and Pkh2 Differentially Phosphorylate and Activate Ypk1 and Ykr2 and Define Protein Kinase Modules Required for Maintenance of Cell Wall Integrity. *Molecular Biology of the Cell*. 13:3005-3028.

Rutherford, J.C., Y.S. Bahn, B. van den Berg, J. Heitman, and C. Xue. 2019. Nutrient and Stress Sensing in Pathogenic Yeasts. *Front Microbiol*. 10:442.

Sanz, M., F. Castrejón, A. Durán, and C. Roncero. 2004. Saccharomyces cerevisiae Bni4p directs the formation of the chitin ring and also participates in the correct assembly of the septum structure. *Microbiology (Reading)*. 150:3229-3241.

Sanz, P., G.R. Alms, T.A. Haystead, and M. Carlson. 2000. Regulatory interactions between the Reg1-Glc7 protein phosphatase and the Snf1 protein kinase. *Mol Cell Biol*. 20:1321-1328.

Seger, S., R. Rischatsch, and P. Philippsen. 2011. Formation and stability of eisosomes in the filamentous fungus Ashbya gossypii. *J Cell Sci*. 124:1629-1634.

Séron, K., M.O. Blondel, R. Haguenauer-Tsapis, and C. Volland. 1999. Uracil-induced down-regulation of the yeast uracil permease. *In* Journal of Bacteriology. Vol. 181. 1793-1800.

Spira, F., N.S. Mueller, G. Beck, P. Von Olshausen, J. Beig, and R. Wedlich-Söldner. 2012. Patchwork organization of the yeast plasma membrane into numerous coexisting domains. *Nature Cell Biology*. 14:640-648.

Steensma, H.Y., J.C. Crowley, and D.B. Kaback. 1987. Molecular cloning of chromosome I DNA from Saccharomyces cerevisiae: isolation and analysis of the CEN1-ADE1-CDC15 region. *Mol Cell Biol*. 7:410-419.

StráDalová, V., W. Stahlschmidt, G. Grossmann, M. BlažÍKová, R. Rachel, W. Tanner, and J. Malinsky. 2009. Furrow-like invaginations of the yeast plasma membrane correspond to membrane compartment of Can1. *Journal of Cell Science*. 122:2887-2894.

Stringer, D.K., and R.C. Piper. 2011. A single ubiquitin is sufficient for cargo protein entry into MVBs in the absence of ESCRT ubiquitination. *The Journal of cell biology*. 192:229-242.

Swaney, D.L., P. Beltrao, L. Starita, A. Guo, J. Rush, S. Fields, N.J. Krogan, and J. Villén. 2013. Global analysis of phosphorylation and ubiquitylation cross-talk in protein degradation. *Nat Methods*. 10:676-682.

Tu, J., and M. Carlson. 1994. The GLC7 type 1 protein phosphatase is required for glucose repression in Saccharomyces cerevisiae. *Molecular and cellular biology*. 14:6789-6796.

Tu, J., and M. Carlson. 1995. REG1 binds to protein phosphatase type 1 and regulates glucose repression in Saccharomyces cerevisiae. *Embo j*. 14:5939-5946.

Vangelatos, I., K. Roumelioti, C. Gournas, T. Suarez, C. Scazzocchio, and V. Sophianopoulou. 2010. Eisosome organization in the filamentous ascomycete Aspergillus nidulans. *Eukaryot Cell*. 9:1441-1454.

Vaskovicova, K., P. Vesela, J. Zahumensky, D. Folkova, M. Balazova, and J. Malinsky. 2020. Plasma Membrane Protein Nce102 Modulates Morphology and Function of the Yeast Vacuole. *Biomolecules*. 10.

Walther, T.C., P.S. Aguilar, F. Fröhlich, F. Chu, K. Moreira, A.L. Burlingame, and P. Walter. 2007. Pkh-kinases control eisosome assembly and organization. *EMBO Journal*. 26:4946-4955.

Walther, T.C., J.H. Brickner, P.S. Aguilar, S. Bernales, C. Pantoja, and P. Walter. 2006. Eisosomes mark static sites of endocytosis. *Nature*. 439:998-1003.

Watanabe, D., R. Kikushima, M. Aitoku, A. Nishimura, I. Ohtsu, R. Nasuno, and H. Takagi. 2014. Exogenous addition of histidine reduces copper availability in the yeast Saccharomyces cerevisiae. *Microb Cell*. 1:241-246.

Weill, U., I. Yofe, E. Sass, B. Stynen, D. Davidi, J. Natarajan, R. Ben-Menachem, Z. Avihou, O. Goldman, N. Harpaz, S. Chuartzman, K. Kniazev, B. Knoblach, J. Laborenz, F. Boos, J. Kowarzyk, S. Ben-Dor, E. Zalckvar, J.M. Herrmann, R.A. Rachubinski, O. Pines, D. Rapaport, S.W. Michnick, E.D. Levy, and M. Schuldiner. 2018. Genome-wide SWAp-Tag yeast libraries for proteome exploration. *Nature methods*. 15:617-622.

Williams-Hart, T., X. Wu, and K. Tatchell. 2002. Protein phosphatase type 1 regulates ion homeostasis in Saccharomyces cerevisiae. *Genetics*. 160:1423-1437.

Zahumenský, J., C. Mota Fernandes, P. Veselá, M. Del Poeta, J.B. Konopka, and J. Malínský. 2022. Microdomain Protein Nce102 Is a Local Sensor of Plasma Membrane Sphingolipid Balance. *Microbiol Spectr*:e0196122.

Zeno, W.F., U. Baul, W.T. Snead, A.C.M. DeGroot, L. Wang, E.M. Lafer, D. Thirumalai, and J.C. Stachowiak. 2018. Synergy between intrinsically disordered domains and structured proteins amplifies membrane curvature sensing. *Nature Communications*. 9:4152.

Zhao, H., A. Michelot, E.V. Koskela, V. Tkach, D. Stamou, D.G. Drubin, and P. Lappalainen. 2013. Membrane-sculpting BAR domains generate stable lipid microdomains. *Cell Rep*. 4:1213-1223.

Ziółkowska, N.E., L. Karotki, M. Rehman, J.T. Huiskonen, and T.C. Walther. 2011. Eisosome-driven plasma membrane organization is mediated by BAR domains. *Nature Structural and Molecular Biology*. 18:854-856.

FIGURES & LEGENDS
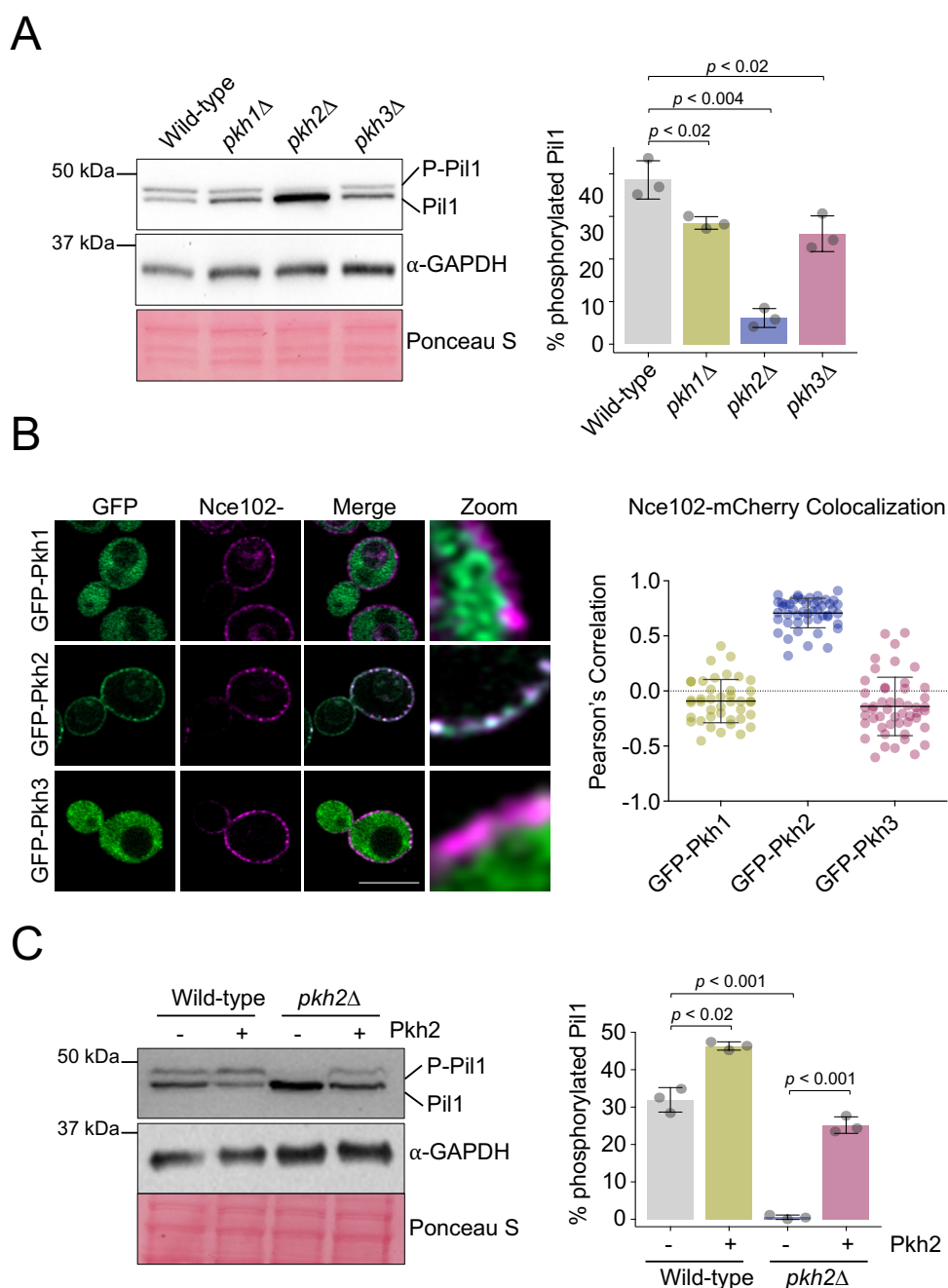
**Figure 1: Pkh2 predominately regulates phosphorylation of Pil1**

A) Whole cell lysates of wild-type, *pkh1Δ*, *pkh2Δ* and *pkh3Δ* cells were analysed by immunoblot using α-Pil1 and α-GAPDH antibodies, with Ponceau S stained membrane included. The percentage phosphorylated Pil1 from each yeast strain was quantified (n=3). **B)** Cells co-expressing Nce102-mCherry and indicated GFP tagged Pkh-kinases were grown to mid-log phase and imaged using confocal microscopy (Airyscan 2). The Pearson's Correlation Coefficient was measured of colocalisation between Nce102-mCherry with the respective GFP-tagged kinases (n > 40). **C)** Wild-type and *pkh2Δ* cells were transformed with either an empty vector control (-) or a 2μ Pkh2 over-expression plasmid (+). Whole cell lysates were generated from transformants and Pil1 phosphorylation assessed by immunoblot. Levels of GAPDH and Ponceau S are shown as loading controls (left). The percentage of phosphorylated Pil1 was quantified (n=3) and shown (right). Statistical significance was determined using Student's *t*-test. Scale bar = 5μm
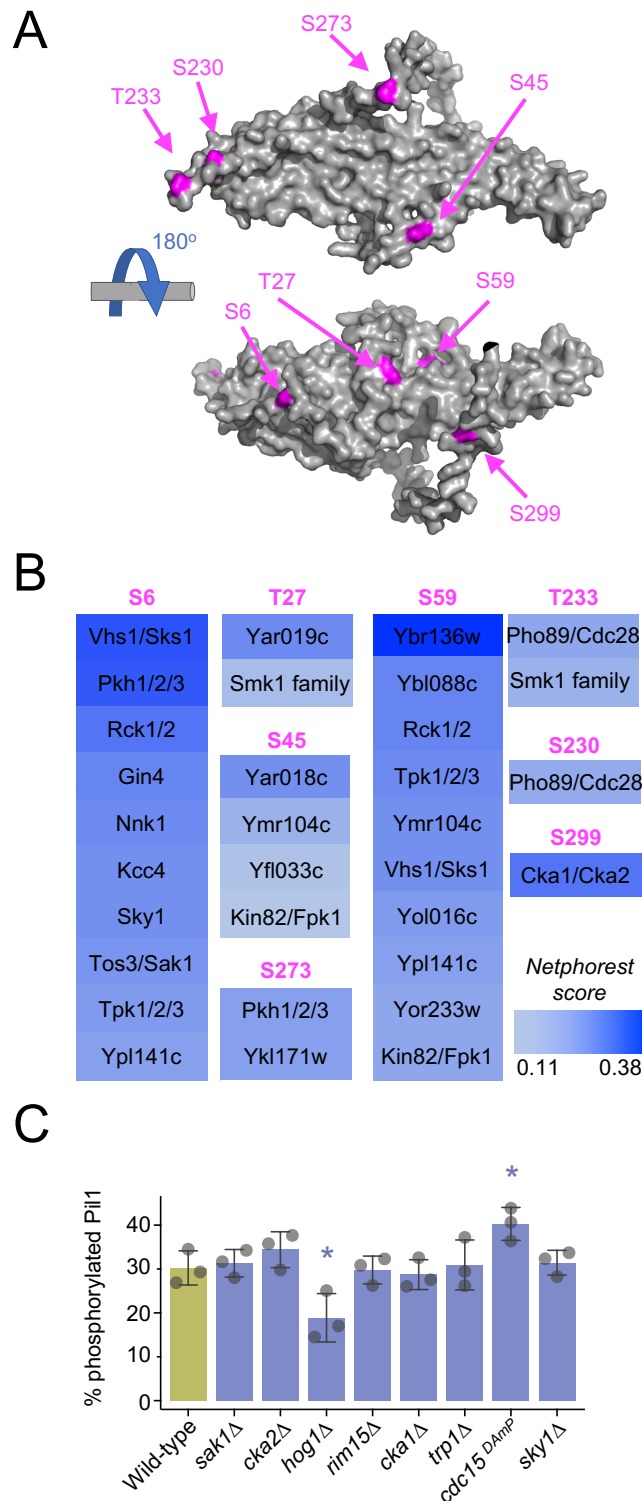
Figure 2: Bioinformatic screen for additional kinases that service Pil1
A) Alphafold structural model of Pil1 residues 1- 307 (grey) shown with eight previously verified phosphorylation sites indicated (magenta). **B)** The Pil1 protein sequence was surveyed using NetPhorest searching against a reference kinase database for *Saccharomyces cerevisiae*. Kinases that scored above threshold (0.1) are presented as a heat map (blue) with the indicated potential phosphorylated residue (magenta). **C)** Whole cell lysates of wild-type and kinase mutant cells were generated and percentage Pil1 phosphorylation assessed by immunoblot and presented as a histogram (n=3).
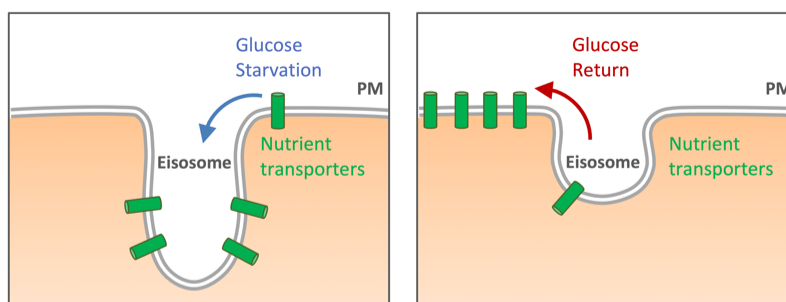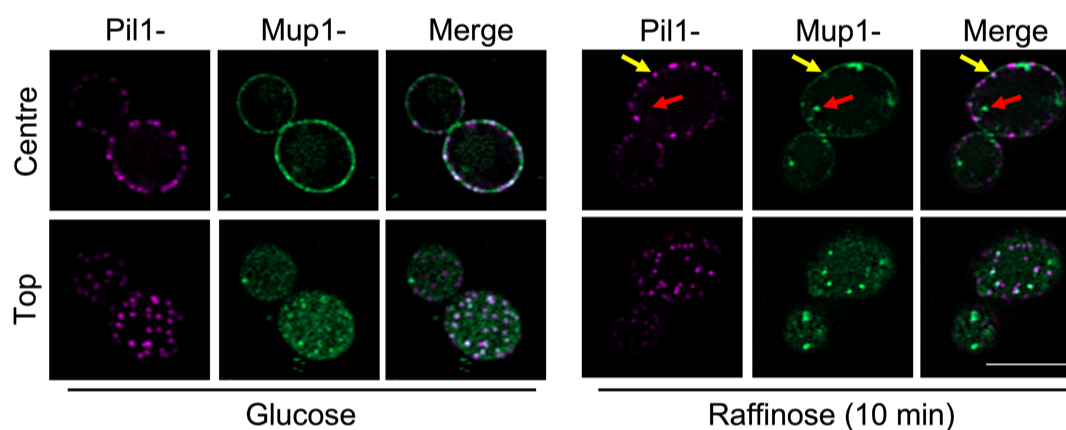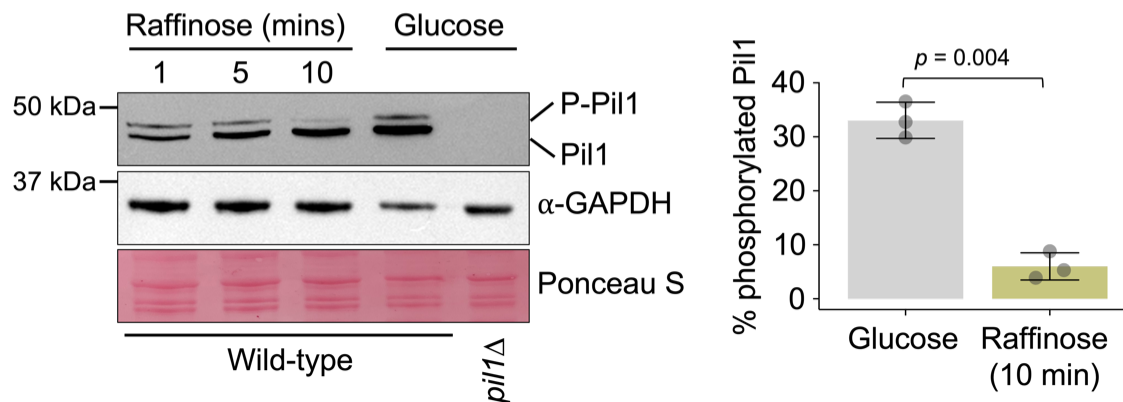
**Figure 3: Pil1 is dephosphorylated in response to glucose starvation**
A) Schematic showing the increased diffusion of nutrient transporters into eisosomes in response to glucose starvation, and their potential exit upon a return to replete nutrient conditions to aid recovery. **B)** Cells co-expressing Pil1-mCherry and Mup1-GFP were imaged using confocal microscopy (Airyscan 2) with centre and top focus under glucose conditions and following 10 minutes of exchange with raffinose media. Mup1 localised to endosomes (red arrow) and Pil1 marked eisosomes (yellow arrow) after raffinose treatment are indicated. **C)** Wild-type cells exposed to raffinose media for 1, 5 and 10 minutes prior to lysate generation were immunoblotted using α-Pil1 antibodies and compared to wild-type and *pil1Δ* cells grown in glucose replete conditions. GAPDH blot and Ponceau S stained membrane is included as a loading control. Percentage of phosphorylated Pil1 was generated for WT vs 10 minutes of raffinose treatment for wild-type cells was quantified (right).
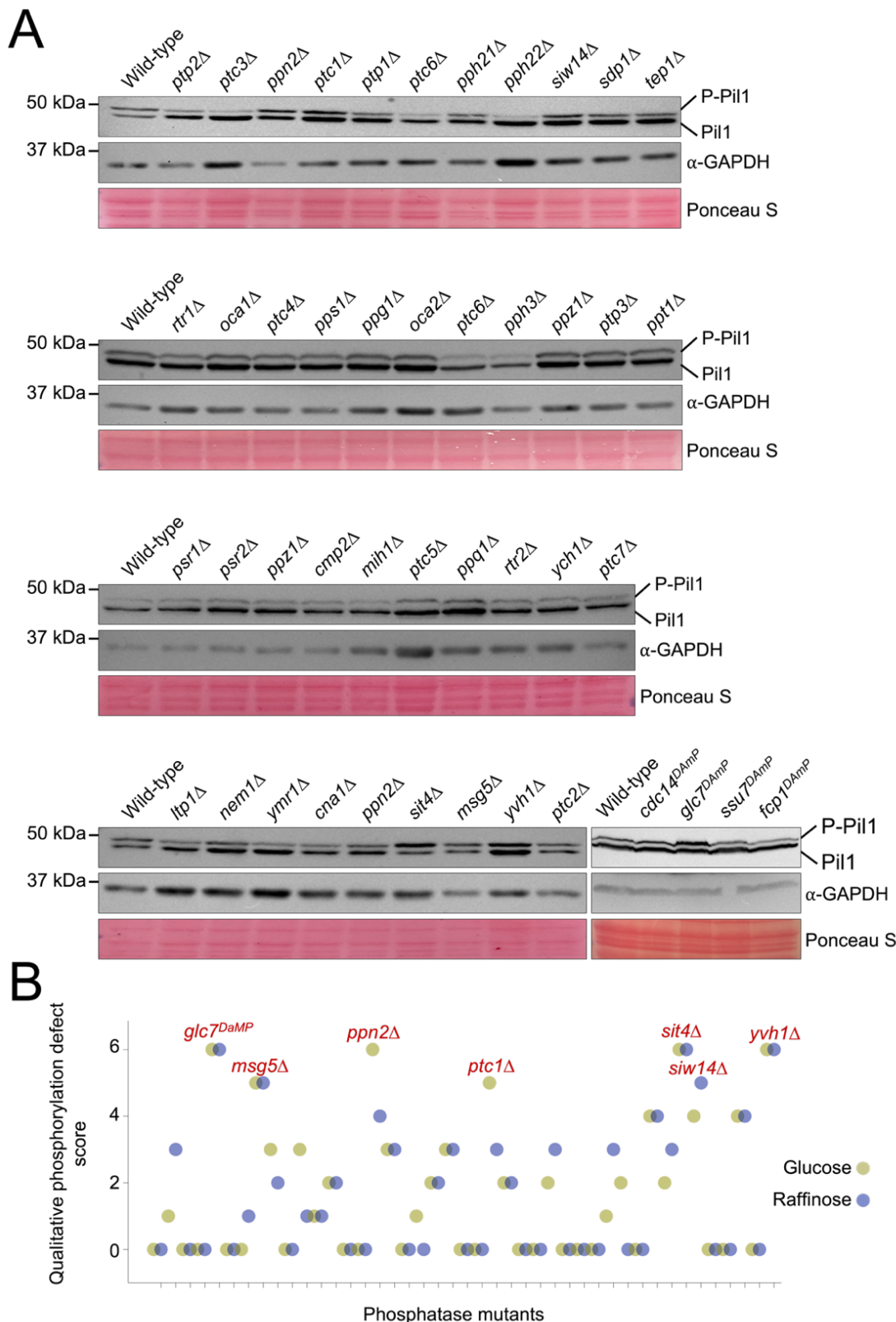
Figure 4: Screen for regulators of Pil1 dephosphorylation
A) Wild-type cells and indicated phosphatase mutants were grown to log-phase in glucose replete conditions prior to lysate generation and immunoblotting with α-Pil1 and α-GAPDH antibodies. Representative blots for at least one mutant are shown, alongside Ponceau S stained membrane. **B)** Immunoblots for all phosphatase mutants were qualitatively scored based on their Pil1 phosphorylation phenotype in both glucose (green) and raffinose (purple) conditions compared with wild-type controls. The highest scoring mutants are labelled in red.
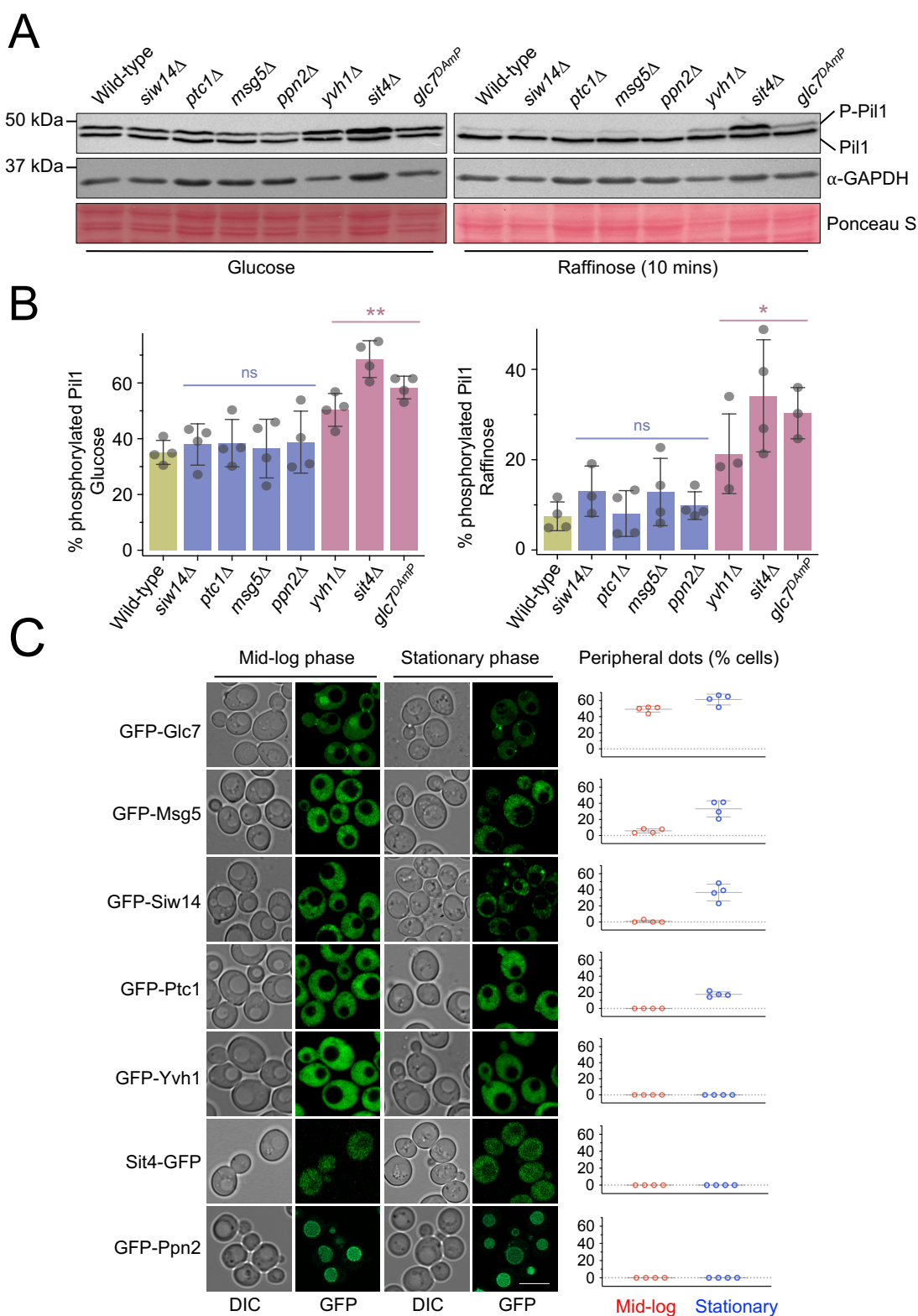
Figure 5: Activity and localisation screens implicate Glc7 in Pil1 regulation
A) Whole cell lysates of wild-type and phosphatase mutant candidates from glucose replete media (left) or following 10 minutes exchange with raffinose media were generated and analysed by immunoblotting using α-Pil1and α-GAPDH antibodies. **B)** Quantification of percentage of Pil1 phosphorylated in indicated mutants was calculated. Statistical significance was determined using Student's t-test. **C)** Yeast expressing GFP tagged phosphatases were cultured to mid-log and stationary phase prior to confocal microscopy (Airyscan). The number of peripheral dots per cell (n > 30) from separate experiments (n = 4) were quantified in each condition (right). Scale bar = 5 μm.
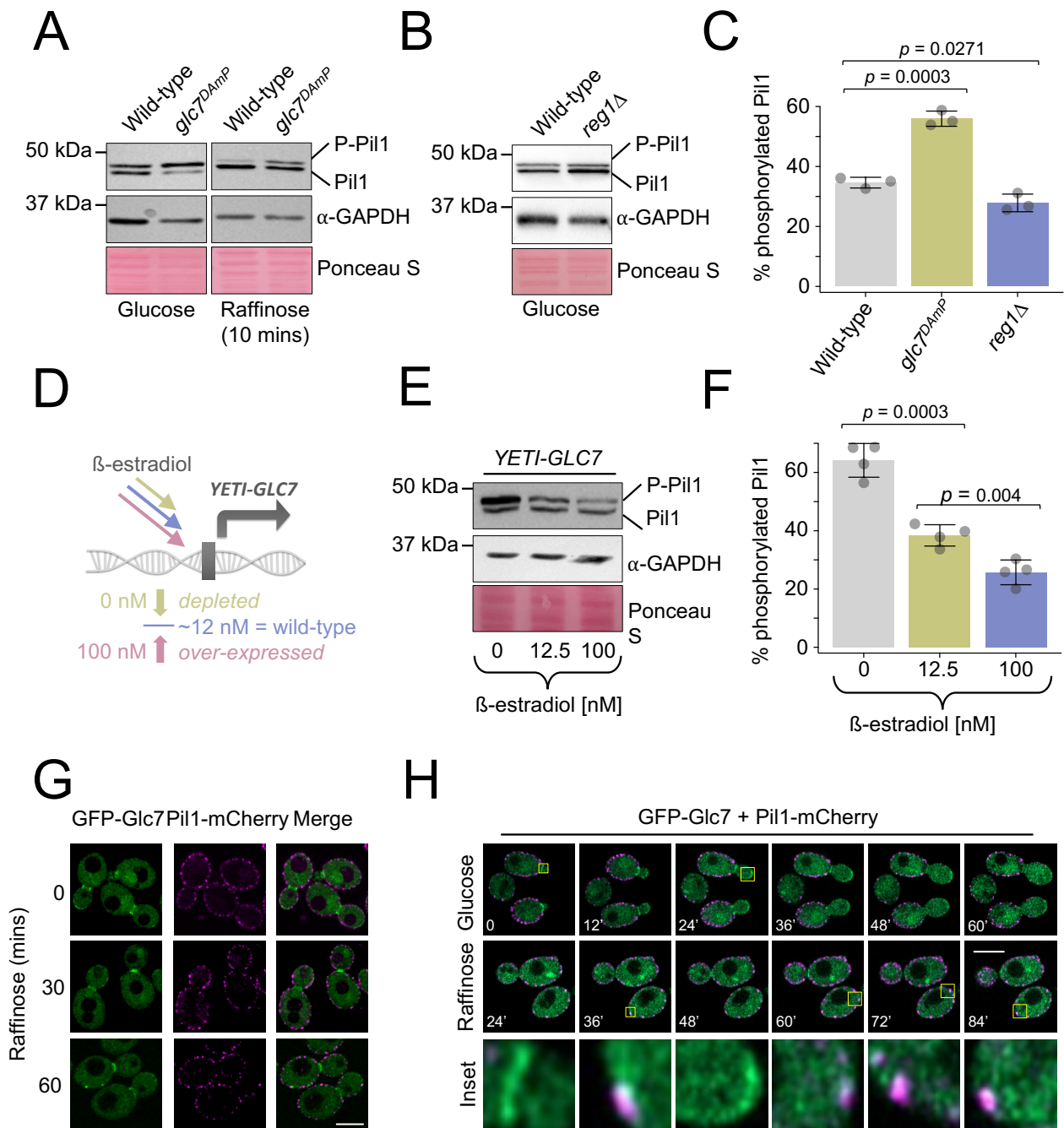
**Figure 6: Glc7 regulates Pil1 dephosphorylation in a Reg1 independent manner**
A) Wild-type and *glc7^DAmP* cells were cultured in glucose media and following 10 minutes of raffinose treatment prior to the generation of whole cell lysates and immunoblotting with α-Pil1 and α-GAPDH antibodies. **B)** Whole-cell lysates of wild-type and *reg1Δ* cells were generated for α-Pil1 and α-GAPDH immunoblot. **C)** The percentage of phosphorylated Pil1 from experiments in A and B was quantified (n=3) and p values from Student's *t*-tests indicated. **D)** Schematic outlining the principle of the YETI expression system for titratable expression of *GLC7* to mimic severely depleted (green) and over-expressed (pink) levels. **E)** *YETI-GLC7* cells were grown overnight in 12.5 nM β-estradiol before washing x3 in YPD media and dilution in fresh media containing 0, 12.5 nM and 100 nM β-estradiol. Cells were then grown for 6 hours prior to the generation of whole-cell lysates and immunoblots using α-Pil1 and α-GAPDH antibodies. **F)** Pil1 phosphorylation was quantified (n=3) from β-estradiol titrations shown in E with p values from Student's *t*-tests shown. **G)** Cells co-expressing GFP-Glc7 and Pil1-mCherry were grown to mid-log phase and imaged using confocal microscopy at 0, 30 and 60 minutes of raffinose treatment. **H)** Time-lapse microscopy of GFP-Glc7 and Pil1-mCherry expressing cells was performed in glucose and 25 minutes raffinose conditions. Scale bar = 5μm.
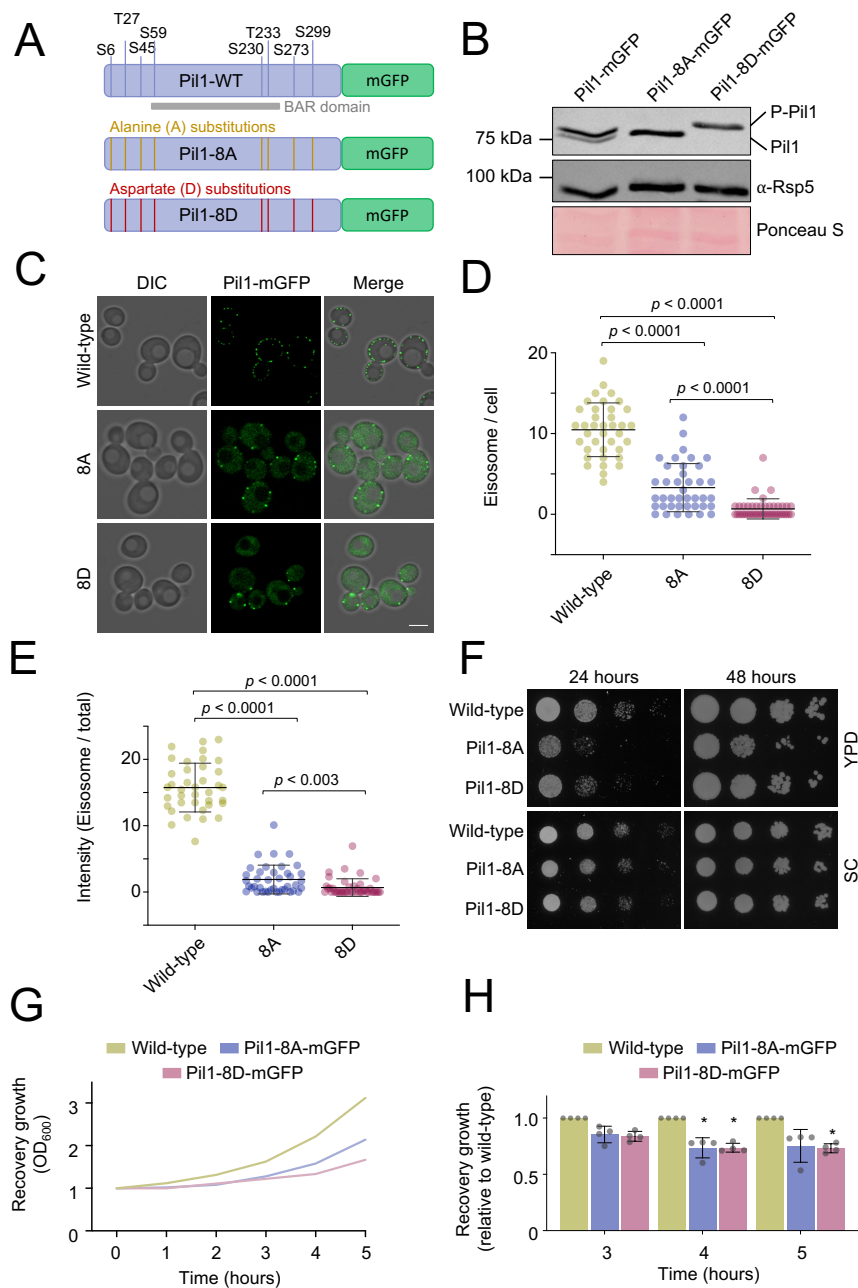
Figure 7: Phosphomutants of Pil1 are defective in starvation recovery

A) Cartoon showing Pil1 fusion to mGFP, including its verified phosphosites and BAR domain. Pil1 cassettes that have been mutated to alanine (yellow) or aspartate (red) that were stably integrated at the *PIL1* locus are also shown. **B)** Pil1 or indicated 8A and 8D mutants were expressed from the endogenous locus as mGFP fusions in strains grown to mid-log phase, harvesting and lysate generation for immunoblotting with α-Pil1 and α-GAPDH antibodies. **C)** Versions of mGFP tagged Pil1 were expressed as the sole chromosomal copy and localised by confocal microscopy coupled to Airyscan 2 detector. **D)** Pil1 labelled eisosomes were identified by otsu segmentation and number per cell quantified (n = > 37) with p values generated from Student's *t*-test comparisons. **E)** Integrated density for all GFP tagged Pil1 versions localised to eisosomes identified from segmentation performed in D was calculated as a percentage of the total signal, with Student's *t*-test comparison generated p values shown. **F)** Indicated yeast strains were grown to log phase in either YPD rich media or SC minimal media, equivalent cell numbers were estimated by optical density measurements and harvested. 10-fold serial dilutions were generated, and yeast spotted out on YPD and SC plates. Growth was recorded at 24 and 48 hours. **G)** Cells at mid-log phase were subjected to 2 hours of glucose starvation (raffinose treatment), returned to glucose replete conditions and growth measured over time. **H)** The growth assay in **G** was repeated (n = 4) and the growth relative to wild-type was quantified for each indicated time-point. Statistical significance was determined using a Student's *t*-test.
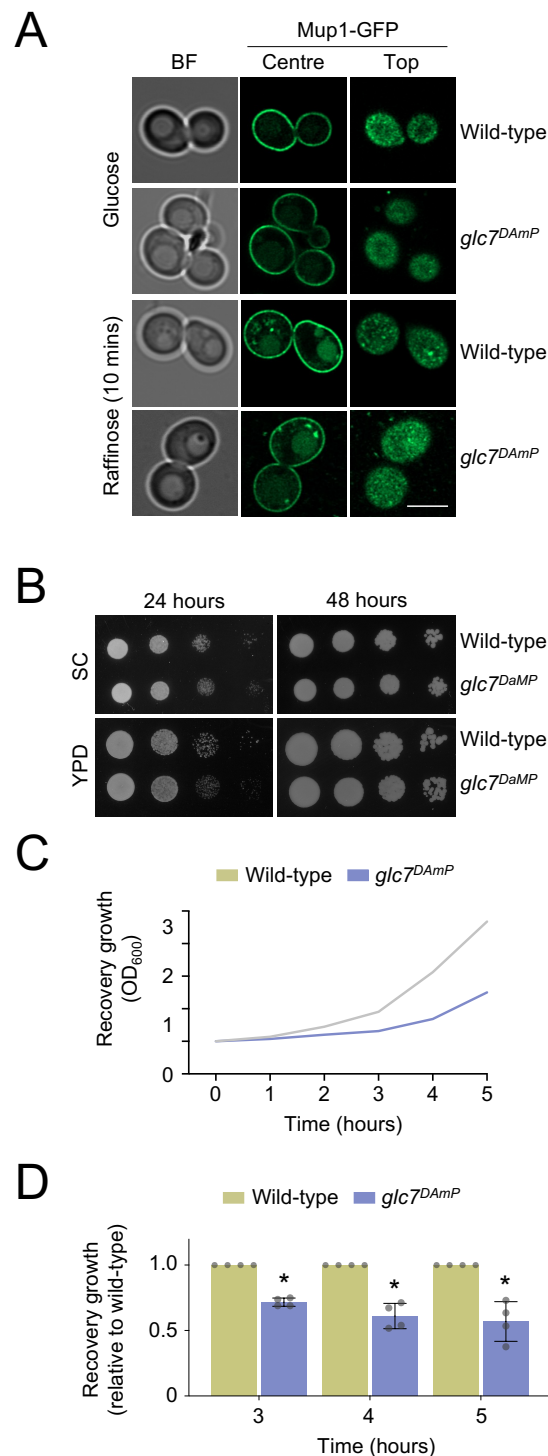
Figure 8: Glc7 is required for efficient recovery from glucose starvation
A) Wild-type and $glc7^{DAmP}$ cells expressing Mup1-GFP were imaged under glucose replete and after 10 minutes Raffinose treatment. Representative images for centre and top focus are shown. Scale bar = 5µm. **B)** Indicated yeast strains were grown to log phase in either YPD rich media or SC minimal media, equivalent cell numbers were estimated by optical density measurements and harvested. 10-fold serial dilutions were generated, and yeast spotted on YPD and SC plates followed by recording growth at 24 and 48 hours. **C)** Cells at mid-log phase were subjected to 2 hours of glucose starvation (raffinose treatment) and then returned to glucose replete conditions where growth was tracked through OD_{600} measurements every hour for 5 hours. **D)** The growth assay in **C** was repeated (n = 4) and the growth relative to wild-type was quantified for each time-point. Statistical significance was determined using a Student's *t*-test.